19. Sandholt, P. E. IMF control of polar cusp and cleft auroras. *Adv. Space Res.* **8,** 21–34 (1988).
20. Newell, P. T. Do the dayside cusps blink? *Rev. Geophys. Suppl.* **33,** 665–668 (1995).
21. Lockwood, M. *et al.* IMF control of cusp proton emission intensity and dayside convection: Implications for component and anti-parallel reconnection. *Ann. Geophys.* **21,** 955–982 (2003).
22. Cowley, S. W. H. & Owen, C. J. A simple illustrative model of open flux tube motion over the dayside magnetopause. *Planet. Space Sci.* **37,** 1461–1475 (1989).

Acknowledgements We are indebted to the IMAGE team and J. L. Burch for the design and successful operation of the IMAGE mission.

Competing interests statement The authors declare that they have no competing financial interests.

Correspondence and requests for materials should be addressed to H.U.F. (hfrey@ssl.berkeley.edu).

Emergence of a molecular Bose–Einstein condensate from a Fermi gas

Markus Greiner[1], Cindy A. Regal[1] & Deborah S. Jin[2]

[1]*JILA, National Institute of Standards and Technology and Department of Physics, University of Colorado,* [2]*Quantum Physics Division, National Institute of Standards and Technology, Boulder, Colorado 80309-0440, USA*

The realization of superfluidity in a dilute gas of fermionic atoms, analogous to superconductivity in metals, represents a long-standing goal of ultracold gas research. In such a fermionic superfluid, it should be possible to adjust the interaction strength and tune the system continuously between two limits: a Bardeen–Cooper–Schrieffer (BCS)-type superfluid (involving correlated atom pairs in momentum space) and a Bose–Einstein condensate (BEC), in which spatially local pairs of atoms are bound together. This crossover between BCS-type superfluidity and the BEC limit has long been of theoretical interest, motivated in part by the discovery of high-temperature superconductors[1–10]. In atomic Fermi gas experiments superfluidity has not yet been demonstrated; however, long-lived molecules consisting of locally paired fermions have been reversibly created[11–15]. Here we report the direct observation of a molecular Bose–Einstein condensate created solely by adjusting the interaction strength in an ultracold Fermi gas of atoms. This state of matter represents one extreme of the predicted BCS–BEC continuum.

The basic idea behind this experiment is to start with a Fermi gas that has been evaporatively cooled to a high degree of quantum degeneracy, and adiabatically create molecules with a magnetic-field sweep across a Feshbach resonance. If the molecule creation conserves entropy and the initial atom gas is at sufficiently low temperature T compared to the Fermi temperature T_F, then the result should be a molecular sample with a significant condensate fraction[13,16]. With a relatively slow sweep of an applied magnetic field that converts most of the fermionic atoms into bosonic molecules and an initial atomic gas below $T/T_F = 0.17$, we observe a molecular condensate in time-of-flight absorption images taken immediately following the magnetic-field sweep. The molecular condensate is not formed by any active cooling of the molecules, but rather merely by traversing the predicted BCS–BEC crossover regime.

Our experimental set-up and the procedure used to cool a gas of fermionic ^{40}K atoms to quantum degenerate temperatures have been detailed in previous work[17,18]. In brief, after laser cooling and trapping we evaporatively cool the atoms in a magnetic trap. In order to realize *s*-wave collisions in the ultracold Fermi gas, we use a mixture of atoms in two different spin states. For the final stage of evaporative cooling, the atoms are loaded into an optical dipole trap formed by a single far-red-detuned laser beam. The laser wavelength is $\lambda = 1{,}064$ nm, and the beam is focused to a waist of 15.5 μm. By lowering the depth of the optical trap, we evaporate the atomic gas to temperatures far below the Fermi temperature $T_F = (6N\nu_r^2\nu_z)^{1/3}h/k_B$. Here N is the particle number in each spin state, ν_r and ν_z are the radial and axial trap frequencies, h is Planck's constant, and k_B is Boltzmann's constant. For final radial trap frequencies between $\nu_r = 430$ Hz and 250 Hz and a fixed trap aspect ratio $\nu_r/\nu_z = 79 \pm 15$, we achieve temperatures between $0.36T_F$ and $0.04T_F$. (All temperatures of the Fermi gas given in this work are determined through surface fits to time-of-flight absorption images[18].)

For this work we use a Feshbach resonance, which occurs when the energy of a quasibound molecular state becomes equal to the energy of two free atoms. The magnetic-field dependence of the resonance allows precise tuning of the atom–atom interaction strength in an ultracold gas[19]. Moreover, time-dependent magnetic fields can be used to reversibly convert atom pairs into extremely weakly bound molecules[11–14,20–24]. The particular resonance used here is located at a magnetic field $B_0 = 202.1 \pm 0.1$ G and has a width of $w = 7.8 \pm 0.6$ G (refs 15, 25). The resonance affects collisions between atoms in the two lowest-energy spin states $|f = 9/2, m_f = -7/2\rangle$ and $|f = 9/2, m_f = -9/2\rangle$ of ^{40}K, where f denotes the total atomic angular momentum and m_f the magnetic quantum number.

To create bosonic molecules from the fermionic atoms, we first prepare an equal mixture of atoms in the $m_f = -9/2$ and $m_f = -7/2$ spin states at temperatures below quantum degeneracy. Then we apply a time-dependent sweep of the magnetic field starting above the Feshbach resonance value, where the atom interactions are effectively attractive, and ending below the resonance, where the atom interactions are effectively repulsive. In contrast to our previous work[11], the magnetic-field sweep is not only adiabatic with respect to the molecule creation rate, but also slow with respect to the collision rate and the radial trap frequency[13]. The magnetic field is typically ramped in 7 ms from $B = 202.78$ G to either $B = 201.54$ G or $B = 201.67$ G. With this magnetic-field sweep across the Feshbach resonance we convert between 78% and 88% of the atoms into molecules. To a very good approximation, these molecules have twice the polarizability of the atoms[26] and therefore are confined in the optical dipole trap with the same trapping frequency and twice the trap depth of the atoms. The molecules, which are all in the same internal quantum state, are highly vibrationally excited, very large in spatial extent, and extremely weakly bound. For a magnetic field 0.43 G below the Feshbach resonance ($B = 201.67$ G) the binding energy $\hbar^2/ma^2$ is 8 kHz, where m is the atomic mass and $2\pi\hbar$ is Planck's constant. The molecule size, which we estimate as $a/2$, is $\sim 1{,}650a_0$, where a_0 is the Bohr radius and a is the atom–atom scattering length given by $a = 174a_0[1 + w/(B_0 - B)]$ (ref. 18). At this magnetic field, the molecule size is one order of magnitude smaller than the calculated intermolecular distance.

A critical element of this experiment is that the lifetime of these weakly bound molecules can be much longer than the typical collision time in the gas and longer than the radial trapping period[12–15]. In previous work, we found that the $^{40}K_2$ molecule lifetime increases dramatically near the Feshbach resonance and reaches ~100 ms at a magnetic field 0.43 G below the Feshbach resonance for a peak density of $n_{pk} = 1.5 \times 10^{13}$ cm^{-3} (ref. 15). It is predicted that this increased molecule lifetime only occurs for dimers of fermionic atoms[27]. The relatively long molecule lifetime near the Feshbach resonance allows the atom/molecule mixture to achieve thermal equilibrium during the magnetic-field sweep. Note, however, that the large aspect ratio of the optical trap gives rise to a

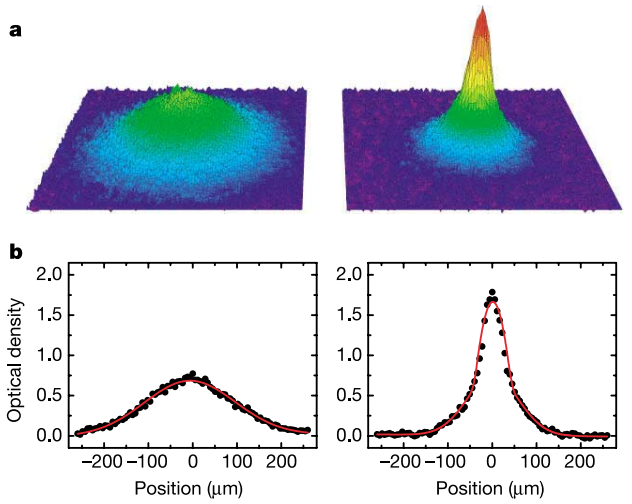

Figure 1 Time-of-flight images of the molecular cloud, taken with a probe beam along the axial direction after 20 ms of free expansion. Data are shown for temperatures above and below the critical temperature for Bose–Einstein condensation. **a**, Surface plot of the optical density for a molecule sample created by applying a magnetic-field sweep to an atomic Fermi gas with an initial temperature of $0.19T_F$ ($0.06T_F$) for the left (right) image. Here the radial trapping frequency of the optical trap was 350 Hz (260 Hz). When we start with the lower initial temperature of the fermionic atoms (right) and ramp across the Feshbach resonance from $B = 202.78$ G to 201.54 G in 10 ms, the molecules form a BEC. During expansion the interparticle interaction was reduced by rapidly moving the magnetic field 4 G further away from the Feshbach resonance. The total molecule number was 470,000 (200,000) for the left (right) picture. The surface plots are the averages of ten images. **b**, Cross-sections through images corresponding to the parameters given above (dots), along with bimodal surface fits (lines). The fits yield no condensate fraction and a temperature of $T = 250\,\text{nK} = 0.90T_c$ for the left graph, and a 12% condensate fraction and a temperature of the thermal component of $T = 79\,\text{nK} = 0.49T_c$ for the right graph. Here, T_c is the calculated critical temperature for a non-interacting BEC in thermal equilibrium.

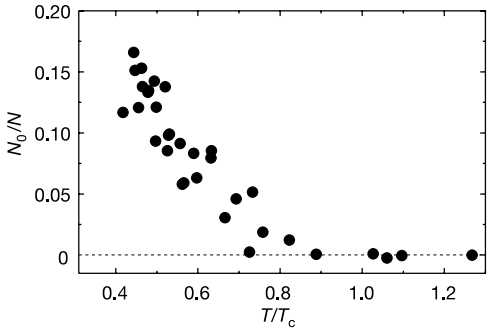

Figure 2 Molecular condensate fraction N_0/N versus the scaled temperature T/T_c. The temperature of the molecules is varied by changing the initial temperature of the fermionic atoms before the formation of the molecules. All other parameters are similar to those described in Fig. 1 legend. We observe the onset for Bose–Einstein condensation at a temperature of $\sim 0.8T_c$; the dashed line marks zero condensate fraction.

strongly anisotropic system. Thus for the relatively short timescale of the experiments reported here we may attain only local equilibrium in the axial direction[28].

To study the resulting atom–molecule mixture after the magnetic-field sweep, we measure the momentum distribution of both the molecules and the residual atoms using time-of-flight absorption imaging. After typically 10–20 ms of expansion, we apply a radio frequency (r.f.) pulse that dissociates the molecules into free atoms in the $m_f = -5/2$ and $m_f = -9/2$ spin states[11]. Immediately after this r.f. dissociation pulse, we take a spin-selective absorption image. The r.f. pulse has a duration of 140 μs and is detuned 50 kHz beyond the molecule dissociation threshold so that it does not affect the residual unpaired atoms in the $m_f = -7/2$ state. We selectively detect the expanded molecule cloud by imaging atoms transferred by the r.f. dissociation pulse into the previously unoccupied $m_f = -5/2$ state. Alternatively, we can image only the expanded atom cloud by detecting atoms in the $m_f = -7/2$ spin state.

Close to the Feshbach resonance, the atoms and molecules are strongly interacting with effectively repulsive interactions. As shown by Petrov *et al.* (ref. 27 and references therein), the scattering length for atom–molecule and molecule–molecule collisions close to the Feshbach resonance are $1.2a$ and $0.6a$ respectively. During the initial stage of expansion, the positive interaction energy is converted into additional kinetic energy of the expanding cloud. Therefore the measured momentum distribution is very different from the original momentum distribution of the trapped cloud. In order to reduce the effect of these interactions on the molecule time-of-flight images, we use the magnetic-field Feshbach resonance to control the interparticle interaction strength during expansion. We can significantly reduce the interaction energy momentum kick by rapidly changing the magnetic field before we switch off the optical trap for expansion. The field is lowered typically by 4 G in 10 μs. At this magnetic field further away from the resonance, a is reduced to $\sim 500a_0$. We find that this magnetic-field jump results in a loss of typically 50% of the molecules, which we attribute to the reduced molecule lifetime away from the Feshbach resonance.

Below an initial temperature of $0.17T_F$, we observe the sudden onset of a pronounced bimodal momentum distribution for the molecules. Figure 1 shows such a bimodal distribution for an experiment starting with an initial temperature of $0.06T_F$; for comparison, we also show the resulting molecule momentum distribution for an experiment starting at $0.19T_F$. The bimodal momentum distribution is a striking indication that the cloud of weakly bound molecules has undergone a phase transition to a BEC[29–31].

To obtain thermodynamic information about the molecule cloud, we fitted the momentum distribution with a two-component fit. The fit function is the sum of an inverted parabola (describing the Thomas–Fermi momentum distribution of a bosonic condensate) and a gaussian momentum distribution (describing the non-condensed component of the molecule cloud). In Fig. 2 the measured condensate fraction is plotted as a function of the fitted temperature of the thermal component in units of the critical temperature for an ideal Bose gas, $T_c = 0.94(N\nu_r^2\nu_z)^{1/3}h/k_B$. Here N is the total number of molecules when there is no change of the magnetic field for the expansion. Note that this measurement may underestimate the original condensate fraction owing to loss of molecules during expansion. From Fig. 2 we determine an actual critical temperature for the interacting molecules and for our trap geometry of $0.8 \pm 0.1T_c$. Such a decrease of the critical temperature relative to the ideal gas prediction is expected owing to repulsive interactions in a trapped gas[32].

We find that the creation of a BEC of molecules requires that the Feshbach resonance be traversed sufficiently slowly. This is illustrated in Fig. 3, where the measured condensate fraction is plotted versus the ramp time across the Feshbach resonance, starting with a Fermi gas at a temperature $0.06T_F$. Our fastest sweeps result in a much smaller condensate fraction, whereas the largest condensate fraction appears for a B-field sweep of 3–10 ms. For even slower magnetic-field sweeps, we find that the condensate fraction slowly decreases. We attribute this effect to a finite lifetime of the condensate. Note that the timescale of the experiment is short compared to the axial trap frequency. Therefore the condensate may not have global phase coherence in the axial direction[28]. The inset of

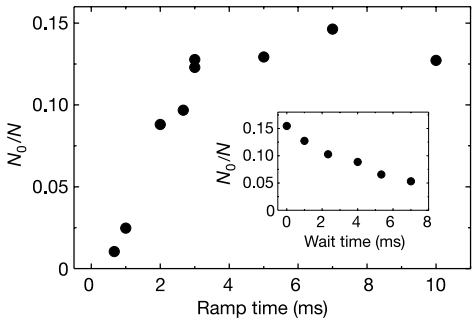

Figure 3 Dependence of condensate formation on magnetic-field sweep rate and measurement of condensate lifetime. We plot the fraction of condensed molecules versus the time in which the magnetic field is ramped across the Feshbach resonance from 202.78 G to 201.54 G. The condensate fraction is measured after an additional waiting time of 1 ms. The initial atom gas temperature is $0.06T_F$, the total molecule number is 150,000, and the final radial trap frequency is 260 Hz. For the full range of ramp times the number of molecules created remains constant. Inset, plot of condensate fraction versus the wait time after a 10-ms magnetic-field ramp. The molecule number is not significantly reduced on this timescale, and the lifetime of the condensate is instead determined by a heating rate, which we measure to be 3 ± 1 nK ms^{-1}. This heating rate is presumably due to density-dependent inelastic loss processes.

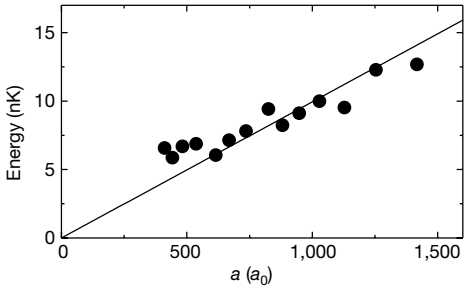

Figure 4 Total expansion energy per particle for the molecular condensate versus the interaction strength during expansion. As the molecular condensate is released from the trap ($\nu_r = 260$ Hz), collisions convert the mean-field interaction energy into kinetic energy of the expanding molecules. In this measurement, the BEC is created in a regime for which we calculate the atom–atom scattering length to be $3{,}300a_0$. For expansion, the magnetic field is rapidly changed to different final values. The graph shows the expansion energy of the condensate fraction determined from a bimodal fit versus the atom–atom scattering length a corresponding to the magnetic field during expansion. The total molecule number is 140,000, the magnetic field before expansion is 201.54 G, and we measure the condensate fraction to be 14%. The line is a linear fit with no offset. We find that the kinetic energy of the condensate molecules is proportional to a.

Fig. 3 shows a plot of the lifetime of the condensate. The observed reduction in condensate fraction is accompanied by heating of the molecule gas, presumably due to the density-dependent collisional decay of molecules into more tightly bound states.

Rapidly changing the interaction strength for time-of-flight expansion of the condensate allows us to measure the interaction energy in the molecular sample. Figure 4 shows a plot of the expansion energy of the molecule BEC for various interaction strengths during time-of-flight expansion. Here the condensate is created at a fixed interaction strength, and thus the initial peak density n_{pk} is constant. The data show that the expansion energy is proportional to a. The linear dependence suggests that the molecule–molecule scattering length is proportional to the atom–atom scattering length, as predicted in ref. 27. In addition, we find that the expansion energy extrapolates to near-zero energy for $a = 0$. This is consistent with a trapped BEC with relatively strong repulsive interactions. Assuming the molecule–molecule interaction strength calculated in ref. 27, this measurement allows us to determine the peak density of the interacting condensate as $n_{pk} = 7 \times 10^{12}$ cm^{-3}.

A fundamental aspect of our experiment is that we start with a quantum degenerate Fermi gas of atoms. The BEC, which is observed immediately after the magnetic field is ramped across the Feshbach resonance, therefore requires a drastic change of the quantum statistical thermodynamics of the gas. This change is not due to evaporative cooling, and the total number of atoms (adding both free atoms and those bound in molecules) is conserved by the field sweep. In Fig. 5 we show the dependence of the condensate fraction on the initial temperature of the Fermi gas. We find that a BEC is formed when the initial temperature is below $0.17T_F$. If we assume that entropy is conserved in the sweep across the Feshbach resonance, then creating the molecular BEC depends on starting with a Fermi gas at sufficiently low T/T_F to give low initial entropy[16]. At the onset of Bose–Einstein condensation, our temperature measurement indicates a modest 40% increase in the total entropy after the magnetic-field sweep, estimated from an ideal gas model. The inset in Fig. 5 compares the absolute temperature of atoms and molecules after the magnetic-field sweep. For the molecules, the temperature is determined by a fit to the non-condensate fraction. We find that atoms and molecules are well thermalized. Note that the atoms and molecules are not in full chemical equilibrium[13]. Even though the final binding energy of the molecules is significantly larger than k_BT, we only observe conversion efficiencies of up to 88%. To study the reversibility of slow ramps (10-ms ramp time) across the Feshbach resonance, we have ramped the magnetic field back to the attractive side of the resonance after creating a molecular condensate and then measured the temperature of the resulting Fermi gas. We find that the gas is heated by 27 ± 7 nK in this double ramp, independent of the initial temperature.

In conclusion, we have created a BEC of weakly bound molecules starting with a gas of ultracold fermionic atoms. The molecular BEC has been detected through a bimodal momentum distribution, and effects of the strong interparticle interaction have been investigated. The molecular BEC reported here, which appears on the repulsive side of the Feshbach resonance, is related in a continuous way to BCS-type fermionic superfluidity on the attractive side of the resonance. Our experiment corresponds to the BEC limit, in which superfluidity occurs owing to Bose–Eistein condensation of essentially local pairs whose binding energy is much larger than the Fermi energy. The dimensionless parameter $1/k_Fa$, which drives the crossover from a BCS-superfluid to a molecular BEC[4,5], is thus

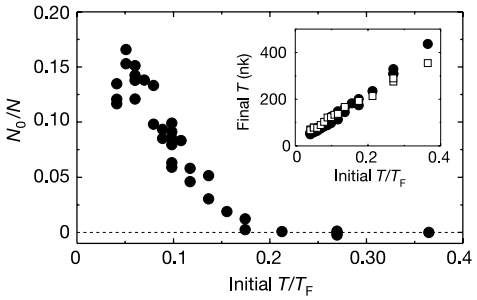

Figure 5 Dependence of the condensate fraction and the temperature of the atom–molecule mixture on the initial scaled temperature T/T_F of the Fermi gas. The condensate fraction is plotted versus T/T_F of the fermionic atoms before the magnetic sweep. In the inset, the temperature of the atoms (open boxes) and the thermal fraction of the molecules (closed circles) are plotted versus T/T_F before the sweep. This is the same data set as in Fig. 2; the dashed line marks zero condensate fraction.

positive and large compared to one. In contrast, near the Feshbach resonance where $1/k_F a$ goes through zero, the system may be described neither by a BEC of molecular dimers nor by a BCS-state of correlated pairs in momentum space, a situation which has been termed 'resonance superfluidity'[6]. Indeed, our experiment passes through this unexplored crossover regime, and with initial temperatures below $0.1T_F$ the Fermi gas is well below the predicted critical temperature in the crossover regime of $0.52T_F$ (ref. 10). In future work, it will be interesting to investigate this system on the attractive side of the resonance and look for evidence of fermionic superfluidity. □

Received 3 November; accepted 14 November 2003; doi:10.1038/nature02199.
Published online 26 November 2003.

1. Leggett, A. J. Cooper pairing in spin-polarized Fermi systems. *J. Phys. C (Paris)* **41,** 7–19 (1980).
2. Nozieres, P. & Schmitt-Rink, S. Bose condensation in an attractive fermion gas: From weak to strong coupling superconductivity. *J. Low-Temp. Phys.* **59,** 195–211 (1985).
3. Drechsler, M. & Zwerger, W. Crossover from BCS-superconductivity to Bose-condensation. *Ann. Phys.* **1,** 15–23 (1992).
4. Haussmann, R. Properties of a Fermi-liquid at the superfluid transition in the crossover region between BCS superconductivity and Bose-Einstein condensation. *Phys. Rev. B* **49,** 12975–12983 (1994).
5. Randeria, M. in *Bose-Einstein Condensation* (eds Griffin, A., Snoke, D. W. & Stringari, S.) 355–392 (Cambridge Univ. Press, Cambridge, UK, 1995).
6. Holland, M., Kokkelmans, S., Chiofalo, M. L. & Walser, R. Resonance superfluidity in a quantum degenerate Fermi gas. *Phys. Rev. Lett.* **87,** 120406 (2001).
7. Timmermans, E., Furuya, K., Milonni, P. W. & Kerman, A. K. Prospect of creating a composite Fermi-Bose superfluid. *Phys. Lett.* **285,** 228–233 (2001).
8. Ohashi, Y. & Griffin, A. BCS-BEC crossover in a gas of Fermi atoms with a Feshbach resonance. *Phys. Rev. Lett.* **89,** 130402 (2002).
9. Milstein, J. N., Kokkelmans, S. & Holland, M. J. Resonance theory of the crossover from Bardeen-Cooper-Schrieffer superfluidity to Bose-Einstein condensation in a dilute Fermi gas. *Phys. Rev. A* **66,** 043604 (2002).
10. Ohashi, Y. & Griffin, A. Superfluid transition temperature in a trapped gas of Fermi atoms with a Feshbach resonance. *Phys. Rev. A* **67,** 033603 (2003).
11. Regal, C. A., Ticknor, C., Bohn, J. L. & Jin, D. S. Creation of ultracold molecules from a Fermi gas of atoms. *Nature* **424,** 47–50 (2003).
12. Strecker, K. E., Partridge, G. B. & Hulet, R. G. Conversion of an atomic Fermi gas to a long-lived molecular Bose gas. *Phys. Rev. Lett.* **91** (2003).
13. Cubizolles, J., Bourdel, T., Kokkelmans, S. J. J. M. F., Shlyapnikov, G. V., Salomon, C. Production of long-lived ultracold Li_2 molecules from a Fermi gas. Preprint at ⟨http://arXiv.org/cond-mat/0308018⟩ (2003).
14. Jochim, S. *et al.* Pure gas of optically trapped molecules created from fermionic atoms. Preprint at ⟨http://arXiv.org/cond-mat/0308095⟩ (2003).
15. Regal, C. A., Greiner, M., & Jin, D. S. Lifetime of molecule-atom mixtures near a Feshbach resonance in ^{40}K. Preprint at ⟨http://arXiv.org/cond-mat/0308606⟩ (2003).
16. Carr, L. D., Shlyapnikov, G. V. & Castin, Y. Achieving a BCS transition in an atomic Fermi gas. Preprint at ⟨http://arXiv.org/cond-mat/0308306⟩ (2003).
17. DeMarco, B. & Jin, D. S. Onset of Fermi degeneracy in a trapped atomic gas. *Science* **285,** 1703–1706 (1999).
18. Regal, C. A. & Jin, D. S. Measurement of positive and negative scattering lengths in a Fermi gas of atoms. *Phys. Rev. Lett.* **90,** 230404 (2003).
19. Stwalley, W. C. Stability of spin-aligned hydrogen at low temperatures and high magnetic fields: New field-dependent scattering resonances and predissociations. *Phys. Rev. Lett.* **37,** 1628–1631 (1976).
20. Donley, E. A., Claussen, N. R., Thompson, S. T. & Wieman, C. E. Atom-molecule coherence in a Bose-Einstein condensate. *Nature* **417,** 529–533 (2002).
21. Chin, C., Kerman, A. J., Vuletic, V. & Chu, S. Sensitive detection of cold cesium molecules formed on Feshbach resonances. *Phys. Rev. Lett.* 033201 (2003).
22. Herbig, J. *et al.* Preparation of a pure molecular quantum gas. *Science* **301,** 1510–1513 (2003).
23. Durr, S., Volz, T., Marte, A. & Rempe, G. Observation of molecules produced from a Bose-Einstein condensate. Preprint at ⟨http://arXiv.org/cond-mat/0307440⟩ (2003).
24. Xu, K. *et al.* Formation of quantum-degenerate sodium molecules. Preprint at ⟨http://arXiv.org/cond-mat/0310027⟩ (2003).
25. Loftus, T., Regal, C. A., Ticknor, C., Bohn, J. L. & Jin, D. S. Resonant control of elastic collisions in an optically trapped Fermi gas of atoms. *Phys. Rev. Lett.* **88,** 173201 (2002).
26. Ratcliff, L. B., Fish, J. L. & Konowalow, D. D. Electronic transition dipole moment functions for transitions among the twenty-six lowest-lying states of Li_2. *J. Mol. Spectrosc.* **122,** 293–312 (1987).
27. Petrov, D. S., Salomon, C. & Shlyapnikov, G. V. Weakly bound dimers of fermionic atoms. Preprint at ⟨http://arXiv.org/cond-mat/0309010⟩ (2003).
28. Shvarchuck, I. *et al.* Bose-Einstein condensation into non-equilibrium states studied by condensate focusing. *Phys. Rev. Lett.* **89,** 270–404 (2002).
29. Anderson, M. H., Ensher, J. R., Matthews, M. R., Wieman, C. E. & Cornell, E. A. Observation of Bose-Einstein condensation in a dilute atomic vapor. *Science* **269,** 198–201 (1995).
30. Davis, K. B. *et al.* Bose-Einstein condensation in a gas of sodium atoms. *Phys. Rev. Lett.* **75,** 3969–3973 (1995).
31. Bradley, C. C., Sackett, C. A. & Hulet, R. G. Bose-Einstein condensation of lithium: observation of limited condensate number. *Phys. Rev. Lett.* **78,** 985–989 (1997).
32. Giorgini, S., Pitaevskii, L. P. & Stringari, S. Condensate fraction and critical temperature of a trapped interacting Bose gas. *Phys. Rev. A* **54,** R4633–R4636 (1996).

Acknowledgements We thank L. D. Carr, E. A. Cornell, C. E. Wieman, W. Zwerger and I. Bloch for discussions, and J. Smith for experimental assistance. This work was supported by NSF and NIST. C.A.R. acknowledges support from the Hertz Foundation.

Competing interests statement The authors declare that they have no competing financial interests.

Correspondence and requests for materials should be addressed to M.G. (markus.greiner@colorado.edu).

Direct observation of Tomonaga–Luttinger-liquid state in carbon nanotubes at low temperatures

Hiroyoshi Ishii[1], Hiromichi Kataura[1], Hidetsugu Shiozawa[1], Hideo Yoshioka[2], Hideo Otsubo[1], Yasuhiro Takayama[1], Tsuneaki Miyahara[1], Shinzo Suzuki[1], Yohji Achiba[1], Masashi Nakatake[3], Takamasa Narimura[4], Mitsuharu Higashiguchi[5], Kenya Shimada[6], Hirofumi Namatame[6] & Masaki Taniguchi[4,6]

[1]*Graduate School of Science, Tokyo Metropolitan University, Minami-Ohsawa 1-1, Hachioji, Tokyo 192-0397, Japan*
[2]*Department of Physics, Nara Women's University, Nara 630-8506, Japan*
[3]*Photon Factory, High Energy Accelerator Research Organization, Tsukuba 305-0801, Japan*
[4]*Graduate School of Science,* [5]*Department of Physical Science,* [6]*Hiroshima Synchrotron Radiation Center, Hiroshima University, Higashi-Hiroshima, 739-8526, Japan*

The electronic transport properties of conventional three-dimensional metals are successfully described by Fermi-liquid theory. But when the dimensionality of such a system is reduced to one, the Fermi-liquid state becomes unstable to Coulomb interactions, and the conduction electrons should instead behave according to Tomonaga–Luttinger-liquid (TLL) theory. Such a state reveals itself through interaction-dependent anomalous exponents in the correlation functions, density of states and momentum distribution of the electrons[1–3]. Metallic single-walled carbon nanotubes (SWNTs) are considered to be ideal one-dimensional systems for realizing TLL states[4–6]. Indeed, the results of transport measurements on metal–SWNT and SWNT–SWNT junctions have been attributed[7–9] to the effects of tunnelling into or between TLLs, although there remains some ambiguity in these interpretations[10]. Direct observations of the electronic states in SWNTs are therefore needed to resolve these uncertainties. Here we report angle-integrated photoemission measurements of SWNTs. Our results reveal an oscillation in the π-electron density of states owing to one-dimensional van Hove singularities, confirming the one-dimensional nature of the valence band. The spectral function and intensities at the Fermi level both exhibit power-law behaviour (with almost identical exponents) in good agreement with theoretical predictions for the TLL state in SWNTs.

The single-particle spectral function $\rho(\omega)$ of TLL states is predicted[1–3] to have a power-law dependence on the binding energy ω near the Fermi energy E_F, ($\rho(\omega) \propto |\omega|^{\alpha}$). As photoemission spectroscopy can directly measure the spectral profile near E_F, photoemission studies on quasi-one-dimensional (1D) conductors and artificial quantum wires have been extensively performed[2,11–17]. In fact, the suppression in photoemission intensity near E_F was observed; many photoemission data suggested that a TLL state may be realized in quasi-1D systems. However, the observed exponents α ($\alpha > 1$) were much larger than the theoretical upper

